



Title	A compound-specific n-alkane $^{13}\text{C}$ and $^{\text{D}}$ approach for assessing source and delivery processes of terrestrial organic matter within a forested watershed in northern Japan
Author(s)	Seki, Osamu; Nakatsuka, Takeshi; Shibata, Hideaki; Kawamura, Kimitaka
Citation	Geochimica et Cosmochimica Acta, 74(2), 599-613 <a href="https://doi.org/10.1016/j.gca.2009.10.025">https://doi.org/10.1016/j.gca.2009.10.025</a>
Issue Date	2010-01-15
Doc URL	<a href="http://hdl.handle.net/2115/42575">http://hdl.handle.net/2115/42575</a>
Type	article (author version)
File Information	GCA74-2_599-613.pdf



[Instructions for use](#)

1  
2  
3 A compound-specific *n*-alkane  $\delta^{13}\text{C}$  and  $\delta\text{D}$  approach for assessing source and  
4 delivery processes of terrestrial organic matter within a forested watershed in  
5 northern Japan  
6  
7  
8

9 Osamu Seki<sup>1\*</sup>, Takeshi Nakatsuka<sup>1,3</sup>, Hideaki Shibata<sup>2</sup> and Kimitaka Kawamura<sup>1</sup>  
10  
11

12 <sup>1</sup>*Institute of Low Temperature Science, Hokkaido University, N19W8, Kita-ku, Sapporo, 060-0819,*  
13 *Japan*  
14

15 <sup>2</sup>*Field Science Center for Northern Biosphere, Hokkaido University, Nayoro, Hokkaido 096-0071,*  
16 *Japan*  
17

18 <sup>3</sup>*Now at Graduate School of Environmental Studies, Nagoya University, Furo-cho, Chikusa-ku,*  
19 *Nagoya 464-8601, Japan*  
20  
21  
22  
23  
24  
25

26 \*Corresponding author (e-mail: seki@pop.lowtem.hokudai.ac.jp, phone: +81-11-706-5504  
27  
28  
29

30 **Running head:**  $\delta^{13}\text{C}$  and  $\delta\text{D}$  of *n*-alkanes in a forested catchment

31 **Index term:** stable carbon isotope, hydrogen isotope, *n*-alkane, riverine organic matter  
32

**32 Abstract**

33 We measured molecular distributions and compound-specific hydrogen ( $\delta\text{D}$ ) and stable  
34 carbon isotopic ratios ( $\delta^{13}\text{C}$ ) of mid- and long-chain *n*-alkanes in forest soils, wetland peats  
35 and lake sediments within the Dorokawa watershed, Hokkaido, Japan, to better understand  
36 sources and processes associate with delivery of terrestrial organic matter into the lake  
37 sediments.  $\delta^{13}\text{C}$  values of odd carbon numbered  $\text{C}_{23}\text{-C}_{33}$  *n*-alkanes ranged from -37.2 to  
38 -31.5 ‰, while  $\delta\text{D}$  values of these alkanes showed a large degree of variability that ranged  
39 from -244 to -180 ‰. Molecular distributions in combination with stable carbon isotopic  
40 compositions indicate a large contribution of C3 trees as the main source of *n*-alkanes in  
41 forested soils whereas *n*-alkanes in wetland soil are exclusively derived from marsh grass  
42 and/or moss. We found that the *n*-alkane  $\delta\text{D}$  values are much higher in forest soils than  
43 wetland peat. The higher  $\delta\text{D}$  values in forest samples could be explained by the enrichment of  
44 deuterium in leaf and soil waters due to increased evapotranspiration in the forest or  
45 differences in physiology of source plants between wetland and forest. A  $\delta^{13}\text{C}$  v.s.  $\delta\text{D}$   
46 diagram of *n*-alkanes among forest, wetland and lake samples showed that  $\text{C}_{25}\text{-C}_{31}$  *n*-alkanes  
47 deposited in lake sediments are mainly derived from tree leaves due to the preferential  
48 transport of the forest soil organic matter over the wetland or an increased contribution of  
49 atmospheric input of tree leaf wax in the offshore sites. This study demonstrates that  
50 compound-specific  $\delta\text{D}$  analysis provides a useful approach for better understanding source  
51 and transport of terrestrial biomarkers in a C3 plant-dominated catchment.

52

## 1. Introduction

52

53 Biomarkers have increasingly become common tools in the reconstruction of past  
54 environmental conditions. Molecular analyses of terrestrial biomarker lipids extracted from  
55 ocean, lake and bog sediments have been used for reconstructions of paleovegetation and  
56 associated paleoclimate histories (e.g., Bird et al., 1995; Ficken et al., 1998; Yamada and  
57 Ishiwatari, 1999; Nott et al., 2000; Xie et al., 2000; Xie et al., 2004; Huang et al., 2001; Seki  
58 et al., 2003; Schefub et al., 2005; Shuman et al., 2006; Zheng et al, 2007; Seki et al., 2009). In  
59 particular, *n*-alkanes have been extensively studied for paleoclimatic purposes. This is  
60 because mid- ( $C_{21}$ - $C_{25}$ ) and long-chain ( $C_{27}$ - $C_{33}$ ) *n*-alkanes, a major component of leaf waxes  
61 and typical biomarkers of vascular plants (Eglinton and Hamilton, 1967), are resistant to  
62 microbial degradation and have been widely found in natural environments including marine  
63 and lacustrine sediments.

64 Molecular distributions and stable carbon isotopic compositions of mid- and long-chain  
65 *n*-alkanes provide powerful paleoclimate information of terrestrial vegetation and climate  
66 (Pancost and Boot, 2004). For instance, average chain length (ACL) and  $P_{aq}$  (% of aquatic  
67 plants) of *n*-alkanes can be used as conventional proxies of continental temperature (Hinrichs  
68 et al., 1998) and source input of aquatic plant derived *n*-alkanes (Ficken et al., 2000),  
69 respectively. The stable carbon isotopic composition ( $\delta^{13}C$ ) of *n*-alkanes has been used to  
70 infer the changes in C3/C4 vegetation where distributions are directly related to climatic  
71 conditions (e.g., Bird et al., 1995; Yamada and Ishiwatari, 1999; Huang et al., 2001; Bendle et  
72 al., 2006; Bendle et al, 2007). Moreover, recently developed techniques for measuring  
73 hydrogen isotope compositions ( $\delta D$ ) of *n*-alkanes has potential as a more direct proxy of  
74 temperature, precipitation, relative humidity and hydrological cycles of the past (e.g., Xie et  
75 al., 2000; Liu and Huang, 2005; Shuman et al., 2006; Hou et al., 2006; Jacob et al., 2007; Seki  
76 et al, 2009).

77 It is generally thought that terrestrial organic components deposited in coastal and lake  
78 sediments near river systems are mainly supplied by river inflows (Goñi, 1997; Goñi et al.,  
79 1997) whereas atmospheric transport of terrestrial materials is a more important delivery  
80 process to pelagic sediments in open ocean and lake center sediments (e.g., Huang et al.,

81 2000; Kawamura et al., 2003; Huang et al., 2006). Terrestrial plant-derived biomarkers  
82 deposited in coastal marine and lacustrine sediments integrate information about terrestrial  
83 ecosystems in catchment basin in the past, but transport processes of organic matter during  
84 fluvial delivery to the sediments are highly variable depending on their phase, that is,  
85 suspended or dissolved forms. Due to a lack of understanding on the delivery and  
86 sedimentation process, paleoclimate applicability of terrestrial biomarkers in marine and  
87 lacustrine sediments is less developed than marine biomarkers (Pancost and Boot, 2004).  
88 Therefore, it is important to understand how fluvial organic materials accumulate in a  
89 catchment basin and how climate records are imprinted in sedimentary deposits for better  
90 application of terrestrial biomarkers in the paleoenvironmental studies of marine and  
91 lacustrine sediments.

92 *n*-Alkanes are often useful for deciphering source and transport information on terrestrial  
93 organic matter in watershed and aquatic environments (Jaffé et al., 1995; Prah1 et al., 1994;  
94 Fernandes and Sicre, 2000; Mead et al., 2005; Seki et al., 2006). Positive correlations  
95 ( $r^2 > 0.88$ ) between concentrations of C<sub>25</sub>-C<sub>31</sub> *n*-alkanes and total organic carbon (TOC) have  
96 been reported in the sediments of river basins (Prah1 et al., 1994; Fernandes and Sicre, 2000),  
97 suggesting that terrestrial plant *n*-alkanes are widely representative biomarkers of fluvial  
98 organic matter input. Isotopic measurements of organic matter are useful for identifying their  
99 sources in natural environments. Because  $\delta^{13}\text{C}$  and  $\delta\text{D}$  in plants are controlled by independent  
100 mechanisms, compound-specific dual isotopic analyses ( $\delta^{13}\text{C}$ - $\delta\text{D}$ ) can provide better source  
101 information on biomarkers than single isotopic analyses (Chikaraishi and Naraoka, 2005;  
102 Chikaraishi et al., 2005; Kurill et al., 2006). In this study, we applied for the first time the  
103 molecular distributions and compound specific stable carbon and hydrogen isotopic  
104 compositions of *n*-alkanes to study the source and transport of terrestrial plant biomarkers in  
105 river water system. Here, we discuss the applicability of this combined approach for  
106 identifying sources and transport processes of terrestrial plant biomarkers in a small  
107 catchment system.

108

109

## 2. EXPERIMENTAL

## 110 **2.1. Sampling site**

111 Hokkaido University's Uryu experimental Forest is located in northern Hokkaido, Japan  
112 (about 44°2N, 142°1E; Fig. 1) and is characterized as a cool temperate forest covered with  
113 broad- and needle-leaf trees and by many streams, ponds and lakes. The total area of the  
114 drainage basin is 3165 ha, total annual rainfall is more than 1000 mm/years and relative  
115 humidity is high (> 75 %) throughout the year. This watershed is characterized by the  
116 presence of a deep snowpack (about 2 m) for a long period (November to May). Fluvial  
117 discharge reaches its maximum in the spring snowmelt season (Ogawa et al., 2006), and the  
118 plant-growing season is restricted to a short summer (June to September). A large amount of  
119 organic rich particulate material is supplied from the Dorokawa river system to Lake  
120 Shumarinai, especially during the snowmelt season. The wetland is a main source of  
121 dissolved organic matter (DOM) in stream water and discharge of DOM via streams plays an  
122 important role in the carbon cycle of the Dorokawa catchment system (Ogawa et al., 2006).

123 In the downstream of the Dorokawa river (altitude of 284-310 m), there are several types  
124 of wetlands while the upstream area is significantly forested (Xiao-niu and Shibata, 2007).  
125 Vegetation in the forest area is characterized by a cool-temperate mixture composed of natural  
126 hardwood and conifer species, mainly represented by Sakhalin fir (*Abies sachalinensis*),  
127 Mongolian oak (*Quercus crispula*), Japanese Manchurian ash (*Fraxinus mandshurica* var.  
128 *japonica*), Erman's birch (*Betula ermanii*), painted maple (*Acer mono*) and Amur cork-tree  
129 (*Phellodendron amurense*). Deciduous trees dominant at high elevations (the highest at 681  
130 m) while conifer-dominated forests are more developed at low elevations. Deciduous trees are  
131 also distributed through the riparian zone. The forest understory is exclusively dominated by  
132 dwarf bamboo except for some wetland areas and riparian zones. Site D in Fig. 1 is composed  
133 of "spruce swamp forests", which contain sparse but pure stands of spruce with dense thickets  
134 of dwarf bamboos in the understory. This site represents the most extensive type of wetland in  
135 the Dorokawa basin. Sites F and E are typical wetland, mostly covered by grasses, herbs and  
136 mosses.

137 Soils and sediments were taken in June and September 2003. Surface soils and soil cores  
138 (0-90 cm depth) were collected from three sites in the forested and upland areas (Sites A, B

139 and C) (Fig. 1). Vegetation in all sites is composed of deciduous and coniferous trees.  
140 However, deciduous trees dominate over coniferous tree as an overstory at the highest  
141 elevation (Site A), while coniferous trees are more important at the mid (Site B) and low  
142 elevation sites (Site C). Surface peat and peat cores (0-120cm depth) (Sites D, E and F) were  
143 collected in the lowland wetland area of the catchment. Lake surface sediments (0-5 cm  
144 depth) were collected in Lake Shumarinai at the mouth of Dorokawa River (Site G) and at  
145 sites distal to the river mouth (Sites H and I). Forest soil and wetland peat cores were cut  
146 every 10cm except for the Site D peat core, which was cut every 30 cm. All the sample  
147 sections were freeze-dried and stored at -20 °C before analyses. River waters were seasonally  
148 collected at 7 sites (Fig. 1) in the watershed from July 2003 to October 2004 for hydrogen  
149 isotopic analysis.

150

## 151 **2.2. Separation and determination of *n*-alkanes**

152 Lipid class compounds were extracted from the dry samples (0.5-7.0 g) with  
153 dichloromethane/methanol (95:5) using an accelerated solvent extractor (Dionex: ASE 200)  
154 three times at 100°C and 1000 psi (about 69 bar) for 5 min each time. The extracts were  
155 concentrated and then saponified with 1.0 M potassium hydroxide/methanol. Neutral  
156 components were isolated by extraction with *n*-hexane/dichloromethane (10:1). Aliphatic  
157 hydrocarbons were separated from other fractions on a silica gel column by eluting with  
158 *n*-hexane. Subsequently, the aliphatic hydrocarbon fraction was separated into saturated and  
159 unsaturated aliphatic hydrocarbon fractions by silver nitrate-impregnated silica gel (10 wt%)  
160 chromatography for compound-specific  $\delta D$  and  $\delta^{13}C$  measurements of *n*-alkanes. The  
161 saturated fraction was eluted with *n*-hexane, whereas the unsaturated fraction was  
162 subsequently eluted with *n*-hexane/dichloromethane (2:1).

163 *n*-Alkanes were analyzed using a HP6890 GC equipped with an on-column injector,  
164 CPSIL-5 CB fused silica capillary column (60 m length, 0.32 mm i.d., film thickness 0.25  
165  $\mu m$ ) and flame ionization detector (FID). The GC oven temperature was programmed from 50  
166 °C to 120 °C at 30 °C/min and then 120 °C to 310 °C at 5 °C/min. Quantification of lipid  
167 compounds was achieved by GC/FID using an authentic *n*-alkane mixture as an external

168 standard. Each compound was identified by GC/mass spectrometry based on retention times  
169 and mass spectra. A Trace GC equipped with an HP-5MS fused silica capillary column (30 m  
170 length, 0.32 mm i.d., film thickness 0.25  $\mu\text{m}$ ) interfaced directly to a mass spectrometer was  
171 used for indentifying organic compounds. The temperature program for the GC/MS analysis  
172 was the same as the GC/FID analysis.

173

### 174 **2.3. Stable carbon and hydrogen isotope analyses**

175 Compound-specific  $\delta^{13}\text{C}$  values of individual *n*-alkanes were determined using a gas  
176 chromatography-isotope ratio mass spectrometry (GC-IRMS) system, which consists of a HP  
177 6890 GC equipped with a DB-5 fused silica capillary column (30 m  $\times$  0.32 mm i.d., film  
178 thickness 0.25  $\mu\text{m}$ ) and an on-column injector, a combustion interface (Finnigan GC  
179 combustion III), and a Finnigan MAT delta Plus mass spectrometer. The GC oven temperature  
180 was programmed from 50  $^{\circ}\text{C}$  to 120  $^{\circ}\text{C}$  at 30  $^{\circ}\text{C min}^{-1}$ , then 120  $^{\circ}\text{C}$  to 310  $^{\circ}\text{C}$  at 5  $^{\circ}\text{C min}^{-1}$ .  
181 The separated compounds from the GC were introduced on-line to the ceramic tube  
182 combustion reactor (850  $^{\circ}\text{C}$ ) that contained thin CuO and Pt wires. The former wire provides  
183 oxygen and the latter acts as a catalyst. In duplicate analyses of selected samples, standard  
184 deviations for  $\delta^{13}\text{C}$  of *n*-alkanes were found to be within 0.5 ‰ (Table 1).  $\delta^{13}\text{C}$  values are  
185 given in per mil (‰) notation relative to the Peedee Belemnite (PDB).  $\text{C}_{21}$  *n*-fatty acid methyl  
186 ester whose isotopic values were known ( $\delta^{13}\text{C} = -26.2$  ‰,  $\delta\text{D} = -227$  ‰) was coinjected with  
187 the samples as an internal isotopic standard for stable carbon and hydrogen isotopic  
188 measurements of *n*-alkanes.

189 Compound-specific  $\delta\text{D}$  values of individual long-chain *n*-alkanes were determined using  
190 a GC/thermal conversion/IRMS system consisting of a HP 6890 GC connected to a Finnigan  
191 MAT delta Plus XL mass spectrometer. Capillary GC column conditions are equivalent to that  
192 of compound-specific  $\delta^{13}\text{C}$  analysis. Pyrolysis (thermal conversion) of *n*-alkanes to  $\text{H}_2$  was  
193 achieved at 1450  $^{\circ}\text{C}$  in a microvolume ceramic tube. A laboratory standard containing  $\text{C}_{16}$ - $\text{C}_{30}$   
194 *n*-alkanes, varying in concentration over a six-fold range and varying in  $\delta\text{D}$  from -248 to  
195 -42 ‰, was analyzed daily. Analytical accuracy of the laboratory standard was within 5 ‰. In  
196 duplicate analyses of samples, standard deviations for *n*-alkane  $\delta\text{D}$  measurements were within



197 10 ‰ (most samples showed an error within 5 ‰; see Table 1).  $\delta D$  values are given in mil  
198 (‰) notation relative to Standard Mean Ocean Water (SMOW).

199 A concern during hydrogen isotopic measurements is that the reaction ( $H_2^+ + H_2 \rightarrow H_3^+ +$   
200 H) occurs readily in the ion source of the mass spectrometer.  $H_3$  is not resolved from  $HD^+$  by  
201 typical IRMS. After correcting for the contribution of  $H_3^+$  to the mass-3 beam (Sessions et al.,  
202 2001), the D/H ratios of *n*-alkanes can be calculated by integrating the mass-2 and mass-3  
203 signals. The  $H_3^+$  factor was determined by observing changes in the (mass-3)/(mass-2)  
204 ion-current ratio since the pressure of  $H_2$  in the ion source chamber was varied by adjustment  
205 of the variable-volume inlet.

206  $\delta D$  of river water was measured using an IsoPrime PyrOH system (GV-instruments), in  
207 which  $H_2O$  is converted to  $H_2$  gas by the chromium-reduction method at 1050 °C and  
208 introduced into an isotopic ratio mass spectrometer together with the He carrier gas. At the  
209 beginning of measurements on a given day, two kinds of standard water were analyzed to  
210 determine the SMOW/SLAP scale. Each water sample was measured in triplicate and the  
211 standard water also analyzed every 10 samples to account for instrument drift of  $\delta D$  values.  
212 The analytical precision (1s) in triplicate measurements is about 0.5 ‰.

213  
214

### 3. RESULTS AND DISCUSSION

#### 3.1. Hydrogen isotopic compositions of stream waters

216 Figure 2 shows seasonal changes in  $\delta D$  values of stream waters in Dorokawa catchment  
217 sites 1, 4, 6, 10, 13 16 and 20. The seasonal variations in  $\delta D$  values are characterized by a  
218 maximum in summer to autumn (August to October) and minimum in spring (April and May)  
219 when snow starts to melt (Ogawa et al., 2006). Thus, the spring minimum  $\delta D$  was likely  
220 caused by an increased contribution of the melt water, whose  $\delta D$  values are always lower than  
221 that of summer precipitation in boreal regions such as Hokkaido (Dansgaard, 1964). However,  
222 the variations are rather small at all sites, ranging from -81 ‰ to -72 with an annual mean  $\delta D$   
223 value of -75‰. Isotopic differences among sites are within 5 ‰ throughout the observation  
224 period, which is smaller than the range of seasonal variability. This result indicates that

225 spatiotemporal differences in the isotopic composition of environmental water are small  
226 (~8 ‰) in the Dorokawa catchment basin.

227

### 228 **3.2. Concentrations and molecular distributions**

229 Figure 3 shows typical molecular distributions of *n*-alkanes in surface layer samples at  
230 each site in Dorokawa catchment and Lake Shumarinai. As evidenced from ACL (ranging  
231 from 27.7 to 30.9; Table 1), the main components of the *n*-alkanes are medium- and  
232 long-chain *n*-alkanes (from C<sub>23</sub> to C<sub>33</sub> *n*-alkanes) in all sites. All samples show a strong odd to  
233 even carbon number predominance. Carbon preference indices (CPI) of *n*-alkanes (Bray and  
234 Evans, 1961) varied between 4.4 and 13.7. These characteristics demonstrate that *n*-alkanes in  
235 the soils, peats and sediments are largely originated from vascular higher plants.

236 Concentrations of total *n*-alkanes range from 4.6 to 435.0 μg/g in all samples. In general,  
237 concentrations are significantly higher in wetland peats than in the forest soils and lake  
238 sediments. Larger amounts of *n*-alkanes in wetland peat probably reflects to greater  
239 preservation of organic matter under anoxic conditions compared to the forested soil where  
240 microbial degradation of organic matter occurs largely under aerobic conditions.

241 A number of studies have reported that the molecular distributions of *n*-alkanes  
242 significantly depend on plant species and the environments where plants grow (Cranwell,  
243 1973; Rieley et al., 1991; Ficken et al., 2000; Nott et al., 2000; Baas et al., 2000; Bi et al.,  
244 2005; Sachse et al., 2006; Nichols et al., 2006; Rommerskirchen et al., 2006). Previous  
245 studies have shown that molecular distributions of *n*-alkanes in non-emergent (submerged and  
246 floating) aquatic plants are characterized by a predominance of medium-chain lengths such as  
247 C<sub>23</sub> and C<sub>25</sub>, while those of terrestrial plants are dominated by long-chain homologues (>C<sub>29</sub>)  
248 (Ficken et al., 2000). Emergent aquatic plants have *n*-alkane distributions midway between  
249 non-emergent and terrestrial plants. Based on modern plant-leaf wax data, Ficken et al. (2000)  
250 defined a new proxy; that is,  $P_{aq} = (C_{23}+C_{25})/(C_{23}+C_{25}+C_{29}+C_{31})$ , which approximates the  
251 proportion of submerged and floating aquatic macrophyte inputs relative to emergent and  
252 terrestrial plant inputs to lake sediments. It has also been reported that *Sphagnum* species

253 show molecular distributions similar to submerged plants, being characterized by a  
254 dominance of  $C_{23}$  and/or  $C_{25}$  *n*-alkanes (Ficken et al., 1998; Baas et al., 2000; Nott et al. 2000;  
255 Nichols et al., 2006). Several studies have reported that *n*-alkane distributions of trees, shrubs,  
256 and emergent water plants tend to show large proportions of the  $C_{27}$  *n*-alkane (Rieley et al.,  
257 1991; Ficken et al., 2000; Bi et al., 2005; Sachse et al., 2006), whereas those of  $C_3$  grasses are  
258 generally dominated by the  $C_{31}$  *n*-alkane (Cranwell, 1973; Bi et al., 2005; Rommerskirchen et  
259 al., 2006).

260 In general, *n*-alkane distributions in all forested soils (Sites A, B and C) are characterized  
261 by a peak at  $C_{29}$  or  $C_{31}$ .  $P_{aq}$  and  $C_{27}/C_{31}$  ratios in forest soils range from 0.13 to 0.4 and from  
262 0.2 to 1.25, respectively. These characteristics are typical of terrestrial tree leaf waxes,  
263 suggesting they represent an important source of *n*-alkanes in soils. In contrast, wetland  
264 samples (Sites D, E and F) showed variable molecular distributions, being different from  
265 forest soil samples. For instance, samples from Sites D and F are characterized by a  
266 pronounced  $C_{31}$  peak and relatively low  $C_{27}/C_{31}$  ratio (0.07-0.28). The low  $C_{27}/C_{31}$  ratios at  
267 Sites D and F are consistent with the wetland vegetations dominated by  $C_3$  grass (Cranwell,  
268 1973; Bi et al., 2005; Rommerskirchen et al., 2006). Molecular distributions at Site E that are  
269 remarkably different from the other sites (Fig. 3), are characterized by relatively high  $P_{aq}$   
270 values (0.22-0.44) and a bimodal distribution with two peaks at  $C_{25}$  and  $C_{31}$ , suggesting a  
271 significant input of submerged plants or *Sphagnum* species as well as grasses. Given that  
272 *Sphagnum* species are one of the main vegetation types in wetland Site E, the  $C_{23}$  and  $C_{25}$   
273 *n*-alkanes could be derived from *Sphagnum* species. These results suggest that molecular  
274 distributions of *n*-alkanes in surface soil samples presented here generally reflect main  
275 vegetation types at each site. On the other hand, molecular distributions of *n*-alkanes in lake  
276 sediments (Sites G, H and I) are characterized by relatively low ACL values (<29) and high  
277  $C_{27}/C_{31}$  ratios (0.87-1.62) compared to other sites. The high  $C_{27}/C_{31}$  ratio suggests a greater  
278 contribution from tree leaf-derived waxes rather than grasses and aquatic plants.

279 The molecular distributions and concentrations of *n*-alkanes also vary significantly with  
280 depth in both forest and wetland samples (Fig. 4). In forested soils, some profiles seem to  
281 have a relationship with depth. In particular, remarkable changes with depth are observed in

282 concentrations and the  $C_{27}/C_{31}$  ratios of *n*-alkanes that are relatively high in surface soils, but  
283 decreased substantially with depth at all sites (Fig. 4a and 4d). CPI and ACL values also show  
284 increases with depth at Sites B and C. In contrast to forested soils, concentrations and  
285 molecular distributions in wetland samples do not show any increase or decrease with depth  
286 except for Site E where CPI,  $C_{27}/C_{31}$  and  $P_{aq}$  show a decreasing trend with depth.

287 Down core profiles of *n*-alkanes at Sites A-C and E possibly result from alternation of  
288 *n*-alkanes during early diagenesis and/or changes in vegetation in the past. In the forest area,  
289 the decreases in concentration down the soil profiles are apparently a result of the degradation  
290 of *n*-alkanes during early diagenesis. Similar depth profiles have been reported in three types  
291 of soil collected from British uplands (Huang et al., 1996). Decreasing ACL and  $C_{27}/C_{31}$  with  
292 depth is probably largely due to preferential degradation of low molecular weight *n*-alkanes in  
293 the soils rather than changes in vegetation in the past. In a study of Scandinavian peat, it has  
294 been found that, in parallel with humification, the major *n*-alkane homologue changed from  
295  $C_{25}$  and  $C_{27}$  to  $C_{31}$ , suggesting selective removal of shorter chain *n*-alkanes in the humification  
296 process (Lehtonen and Ketola, 1993). In contrast, the down-core profile of molecular  
297 distributions in the wetland sites (D and F) largely reflects changes in input of vegetation in  
298 the past rather than diagenetic alternation, given the greater preservation potential of organic  
299 matter in wetlands due to anoxic conditions. The large amounts of *n*-alkanes at all depths in  
300 the wetland cores suggest that, although the wetland area is smaller than the forested area, it  
301 represents an important reservoir of *n*-alkanes in the catchment area.

302

### 303 **3.3. Compound-specific stable carbon and hydrogen isotopic compositions**

304 The stable carbon isotopic signature of terrestrial plants largely depends on carbon  
305 fixation pathway, but is also controlled by plant physiology. Bulk  $C_3$  plant tissues have lower  
306 isotopic values ( $\delta^{13}C \approx -25\text{‰}$  to  $-28\text{‰}$ ) while that of  $C_4$  plants have higher values ( $\delta^{13}C \approx$   
307  $-10\text{‰}$  to  $-14\text{‰}$ ) (Smith and Epstein, 1971). Concentrations of atmospheric  $CO_2$ , which  
308 decreases with elevation, also influence the  $\delta^{13}C$  of terrestrial plants. However, since altitude  
309 differences among the sampling sites are small ( $\sim 400$  m) in this study, the effect is negligible.  
310 Studies of numerous plants taken from the local area have shown that the  $\delta^{13}C$  of alkyl lipids

311 in C<sub>3</sub> and C<sub>4</sub> plant are generally ~8 ‰ and ~12 ‰ lighter than those of bulk tissues,  
312 respectively (Collister et al., 1994; Chikaraishi and Naraoka, 2003). It has also been reported  
313 that δ<sup>13</sup>C values are lower in C<sub>3</sub> angiosperms (-38 ~ -32 ‰) than in C<sub>3</sub> gymnosperms (-32 ~  
314 -29 ‰) at single sites (Chikaraishi and Naraoka, 2003; Pedentchouk et al., 2008), reflecting a  
315 difference in plant physiology such as stomatal conductance for CO<sub>2</sub> between the two species.

316 The δD values of plant biomolecules primarily reflect the environmental water that the  
317 plants uptake. δD in environmental water depends on climatic conditions (temperature,  
318 evaporation and precipitation) and varies significantly from -300 to 0 ‰ depending on the  
319 global and local hydrological cycles, and thus biomolecules of plants have almost the same  
320 range of δD as meteoric water (Ehleringer and Rundel, 1989). The δD values of plant  
321 biomolecules are secondarily influenced by kinetic isotopic fractionation during biosynthesis.  
322 Because biosynthesis of *n*-alkane discriminates against deuterium relative to hydrogen  
323 (Sternberg et al., 1984; Sessions et al., 1999), *n*-alkanes in aquatic plants show lower δD  
324 values than their host water by 155-160‰ (Sessions et al., 1999; Huang et al., 2004; Sachse et  
325 al., 2004). Hydrogen isotopic fractionation between environmental water and *n*-alkanes  
326 ( $\epsilon_{n\text{-alkane/water}}$ ) is calculated by the following equation:  $\epsilon_{n\text{-alkane/water}} = (\delta_{n\text{-alkane}} + 1)/(\delta_{\text{water}} + 1) - 1$ .

327 The C<sub>23</sub>-C<sub>33</sub> *n*-alkane δ<sup>13</sup>C values in all sites ranged from -38 to -31 ‰ and most samples  
328 fell in the range expected for C<sub>3</sub> angiosperm leaf wax (Chikaraishi and Naraoka, 2003;  
329 Pedentchouk et al., 2008) (Table 2). This indicates that the main source of long-chain  
330 *n*-alkanes in the soil samples is C<sub>3</sub> angiosperms rather than C<sub>3</sub> gymnosperms. This may  
331 suggest that the *n*-alkane content of angiosperm leaf wax is much greater than that of  
332 gymnosperms.

333 Depth profiles at Site B and C showed that the C<sub>25</sub>-C<sub>31</sub> *n*-alkanes are gradually enriched  
334 in <sup>13</sup>C with depth by up to 3 ‰ (Fig. 5). A similar phenomenon has been reported in other  
335 soils, in which no changes in vegetation types (C<sub>3</sub> vs C<sub>4</sub>) were found in the past (Huang et al.,  
336 1996; Ficken et al., 1998). A 1.3 ‰ change in isotopic enrichment can be explained by recent  
337 depletion of atmospheric δ<sup>13</sup>C due to fossil fuel burning (Keeling et al., 1984). Another 1.7 ‰  
338 may be explained by early diagenesis associated with heterotrophic reworking (Huang et al.,  
339 1996; Ficken et al., 1998; Chikaraishi and Naraoka, 2006) or changed vegetation in the past.

340 On the other hand,  $\delta^{13}\text{C}$  enrichment with increasing depth has not been observed in wetland  
341 sites. This suggests that  $\delta^{13}\text{C}$  variations of peat core sequences largely reflect changes in  $\delta^{13}\text{C}$   
342 of source plants in the past. Although molecular distributions showed distinct differences  
343 between forest and wetland samples, no clear difference was observed in  $\delta^{13}\text{C}$  profiles. A  
344 one-way analysis of variance (ANOVA) shows there is no significant difference between  $\delta^{13}\text{C}$   
345 values of  $\text{C}_{25}\text{-C}_{33}$  *n*-alkanes in forest and wetland ( $P = 0.559$ ). This indicates that the  $\delta^{13}\text{C}$   
346 approach is not sensitive enough to differentiate the sources of organic matter in the  
347 catchments.

348 The  $\delta\text{D}$  values of  $\text{C}_{23}\text{-C}_{33}$  *n*-alkanes in the catchment show a wide range from -186 to  
349 -245 ‰ and are depleted in deuterium relative to environmental waters (-80 ~ -72 ‰) (Table  
350 3 and Fig. 6). The most striking feature of the *n*-alkane  $\delta\text{D}$  values is deuterium enrichment in  
351 the forest samples (-214 ~ -186 ‰) compared to the wetland samples (-250 ~ -210 ‰). In fact,  
352 the one-way ANOVA shows there is a significant difference between  $\delta\text{D}$  values of  $\text{C}_{25}\text{-C}_{33}$   
353 *n*-alkanes in forest and wetland samples ( $P = <0.0001$ ). This indicates that  $\delta\text{D}$  analysis can  
354 potentially differentiate *n*-alkanes between forest soils and wetland peats. The  $\delta\text{D}$  values of  
355  $\text{C}_{25}\text{-C}_{31}$  *n*-alkanes in sediment Sites H and I are -204 to -196 ‰ and fall within the range of  
356 forest soils. However, the  $\delta\text{D}$  values (-219 ~ -214 ‰) in Site G, which is surrounded by  
357 wetland, are rather consistent with the wetland samples. In contrast to the  $\delta^{13}\text{C}$  profile,  
358 enrichment or depletion in deuterium is independent of the *n*-alkane carbon number (Table 3).  
359 Similarly, increasing or decreasing trends with depth are not apparent in the  $\delta\text{D}$  profile of the  
360 *n*-alkanes at soil Site C (Fig. 6).

361 These considerations suggest that early diagenesis does not significantly alter the  $\delta\text{D}$   
362 values of *n*-alkanes in the soil and peat. In fact, a strong propensity for *n*-alkane  $\delta\text{D}$  values to  
363 retain their original isotopic compositions has been suggested by some studies (Yang and  
364 Huang 2003; Dawson et al., 2004). For example, Yang and Huang (2003) compared the  $\delta\text{D}$   
365 compositions of individual *n*-alkanes in the sediment matrix from compressional leaf fossils  
366 in a Miocene (15-20 Ma) paleo-lake deposit. Distinctive  $\delta\text{D}$  patterns of leaf fossils and  
367 sediments indicate that leaf lipids retain their original isotopic compositions. Comparison of  
368  $\delta\text{D}$  values for *n*-alkanes in turbidites (Late Carboniferous to the Late Permian) taken from

369 different climatic locations revealed distinctive latitudinal patterns of  $\delta D$  values with up to  
370 70‰ difference between tropical and high latitudinal sites, suggesting that their indigenous  
371  $\delta D$  signatures have been preserved for 260–280 million years (Dawson et al., 2004).

372

### 373 **3.4. Cause of different $\delta D$ values of *n*-alkanes between forest and wetland**

374 Environmental waters cannot be a major cause for the large variability of *n*-alkane  $\delta D$   
375 values in the Dorokawa watershed, because regional isotopic variations in river waters are  
376 much smaller than the observed differences in the  $\delta D$  values of forest and wetland *n*-alkanes.  
377 Although factors controlling lipid  $\delta D$  values in terrestrial plants are not fully understood,  
378 possible factors that may control *n*-alkane  $\delta D$  values, based on previous studies, are either (1)  
379 differences in  $\delta D$  values of leaf and/or soil waters that reflect micro-climatic gradients or (2)  
380 ecological differences of terrestrial plants.

381 It is expected that relative humidity is higher in the wetland than in the forested area and  
382 the degree of evaporation at soil and leaf surfaces is larger in the forested area than the  
383 wetland, leading to  $\delta D$  enrichment of leaf water in forest plants compared to wetland grasses.  
384 This interpretation is supported by the observational results that  $\delta D$  values of terrestrial plant  
385 lipids, which are exposed to significant evaporation, are  $\sim 30$  ‰ heavier than that of aquatic  
386 plants, which are protected from deuterium enrichment of leaf water (Chikaraishi et al., 2003;  
387 Huang et al., 2004; Sachse et al., 2004).

388 In addition to the difference in humidity, differences in plant life form or plant  
389 physiology may contribute to the observed isotopic variations. The results of leaf wax  
390 *n*-alkane  $\delta D$  measurements from various types of terrestrial plants collected within the same  
391 climatic conditions showed a large variability in lipid  $\delta D$  values among plant types  
392 (Chikaraishi et al., 2003; Liu et al., 2006; Hou et al., 2007). Interestingly, significant higher  
393  $\delta D$  values for tree leaf wax *n*-alkanes were reported compared to those for grasses and herbs  
394 (Liu et al., 2006; Hou et al., 2007). This isotopic difference has been interpreted as a result of  
395 the ecological differences of terrestrial plants, probably leading to different degrees of  
396 evapotranspiration. Hence, the observed difference in  $\delta D$  between wetland and forest sites  
397 may be caused by different plant types (tree vs grass) as suggested by previous studies.

398 Assuming that  $\delta D$  of environmental water is  $-75\text{‰}$  in all sites, apparent hydrogen  
399 isotopic fractionation between environmental water and *n*-alkanes is  $-146$  to  $-123\text{‰}$  in the  
400 forest surface soils and  $-179$  to  $-143\text{‰}$  in the wetland surface peats. The apparent hydrogen  
401 isotopic fractionations in forest samples are lower than the  $\epsilon_{\text{water-alkane}}$  ( $160\text{‰}$ ) between  
402 *n*-alkanes and algae uptake water (Huang et al., 2004; Sachse et al., 2006). This suggests that  
403 there exists an enrichment of environmental water  $\delta D$  by  $15\sim 40\text{‰}$  due to the  
404 evapotranspiration at the interface between air and soil or plant leaf, or there is smaller  
405 biosynthetic fractionation in forest trees than wetland grasses. On the other hand, relatively  
406 high apparent hydrogen isotopic fractionations in the wetland peat suggest that no or less  
407 isotopic enrichment ( $<15\text{‰}$ ) exists under high relative humidity condition in wetlands or  
408 larger biosynthetic fractionation occurs in wetland plants.

409

### 410 **3.5. Delivery processes and sources of sedimentary organic matter in Lake Shumarinai**

411 In order to infer sources of *n*-alkanes in lacustrine sediments, we compared molecular  
412 distributions of the forest and wetland soils to those of lacustrine sediments. Figure 7 displays  
413 a  $P_{\text{aq}}$  v.s.  $C_{27}/C_{31}$  diagram for all the samples studied. In the diagram, the sediment Site G is  
414 plot in the same area as forest soil *n*-alkanes (Sites A and C), implying a greater contribution  
415 of forest soil derived *n*-alkanes to the sediments. However, the location of Sites H and I in the  
416  $P_{\text{aq}}$  v.s.  $C_{27}/C_{31}$  diagram apparently deviates from all the forest and wetland samples. This  
417 deviation may be ascribed to a limited number of soil samples in the Dokokawa catchment. In  
418 general, the chemical composition of soils is heterogeneous. Hence our dataset may be  
419 insufficient to capture all of the potential soil inputs from the catchment to the lake and  
420 suggests the existence of a significant soil reservoir with higher  $C_{27}/C_{31}$  values somewhere in  
421 the catchment.

422 To further assess the sources of sedimentary *n*-alkanes, we plot  $\delta^{13}\text{C}$  and  $\delta D$  values of  
423  $C_{25}\text{-}C_{31}$  odd *n*-alkanes (Fig. 8). Based on the  $\delta^{13}\text{C}$  v.s.  $\delta D$  diagram, we can discriminate the  
424 sources of individual *n*-alkanes in the lake sediments. In contrast to the molecular distribution  
425 approach, hydrogen isotopic analyses allows source discrimination. All the *n*-alkanes from  
426 Sites H and I plot in the same area as forest soil *n*-alkanes (Sites A to C) while *n*-alkane from



427 sedimentary Site G is plot in the group of wetland Sites D to F or on the mixing line between  
428 forest and wetland. Thus, based on the  $\delta^{13}\text{C}$  v.s.  $\delta\text{D}$  diagram, it is suggested that  $\text{C}_{25}\text{-C}_{31}$  odd  
429 *n*-alkanes in Sites H and I could be mainly derived from upstream forest soils. Sedimentary  
430  $\text{C}_{25}\text{-C}_{31}$  odd *n*-alkanes in Site G may be largely contributed from wetland soil in the lower  
431 reaches of the Dorokawa stream system or be associated with both forest and wetland inputs.

432 Therefore, considering the result of compound-specific hydrogen isotopic analyses, we  
433 speculate that the difference in the molecular distributions between lake sediments is due to  
434 limited number of soil samples in the catchment area. In fact, the high  $\text{C}_{27}/\text{C}_{31}$  ratio in offshore  
435 sediments (Sites H and I) suggests that tree leaf wax is a plausible source, being consistent  
436 with the  $\delta\text{D}$  values that clearly exhibit an input of forest tree derived *n*-alkanes in offshore  
437 sites. The similar molecular distribution of Site G to forested soil samples suggests a possible  
438 contribution from several sources to Site G. As shown in Fig. 3, wetland samples show  
439 variable molecular distributions and a mixture of sources may yield molecular distribution  
440 similar to the forest samples. The discrepancy between the isotopic and molecular distribution  
441 approaches highlights the need for compound-specific isotopic analysis to confirm source  
442 evaluation of biomarkers, although molecular distributions could be useful as conventional  
443 source estimates of organic compounds.

444 Our results suggests that delivery processes for long-chain *n*-alkanes are spatially  
445 different along a transect of the sampling sites of lacustrine sediments. What mechanisms  
446 could cause such a spatial distribution of *n*-alkane sources in lacustrine sediments? One  
447 possible explanation is that hydrodynamic sorting of different source materials during  
448 transport (Keil et al., 1994). This mechanism may be invoked in Lake Shumarinai, i.e. the  
449 particulate materials transported from forest area to the lake largely consist of fine clay  
450 minerals and thus are preferentially transported long distances, while coarse organic particles  
451 containing plant debris from the wetland rapidly sink and are deposited in estuaries. A similar  
452 process was recognized in the Mississippi River system in North America (Goñi et al., 1997;  
453 Goñi et al., 1998). They suggested a preferential transport of fluvial organic matter that  
454 originated from grassland soils in the Mississippi River drainage basin to the offshore in the  
455 Gulf of Mexico.

456 Alternatively, it is also possible that relatively high  $C_{27}/C_{31}$  ratios in offshore sites can be  
457 ascribed to a large atmospheric input of tree leaf waxes to local offshore sites (Gagosian and  
458 Peltzer, 1986; Kawamura et al., 2003). Because *n*-alkanes are a major component of  
459 epicuticular waxes, which cover leaf surfaces, *n*-alkanes in leaf surfaces can easily be ablated  
460 by wind and dust. It is generally accepted that plant wax *n*-alkanes can be transported in the  
461 atmosphere to offshore regions. In the forested site, it is expected that ablated waxes will  
462 accumulate in the air, suggesting atmospheric input may be important in addition to fluvial  
463 delivery. However, aerosol samples were not collected in the study area and thus it is difficult  
464 to evaluate the importance of organic aerosol input to the lake sediments. In order to further  
465 assess the delivery processes of *n*-alkanes deposited in the Lake Shumarinai sediments,  
466 further work including the study of leaf waxes and organic aerosols are needed.

467

468

469

## 5. CONCLUSIONS

470 Multi-proxy approaches including  $C_{27}/C_{31}$  and  $P_{aq}$  together with the stable carbon and  
471 hydrogen isotopic composition of *n*-alkanes were for the first time applied to geochemical  
472 samples in the Dorokawa watershed system, northern Japan, to assess sources and delivery  
473 process of terrestrial organic matter. Molecular distributions and stable carbon and hydrogen  
474 isotopic compositions in soils reflect *in situ* vegetation in Dorokawa drainage basin. Based on  
475 the molecular distributions, *n*-alkanes in forest soils are largely suggested to originate from  
476 tree leaves while those in wetland soils are mostly derived from wetland grass and moss.  
477 Stable carbon isotopic compositions of *n*-alkanes showed greater contributions of  $C_3$   
478 angiosperms as a source of *n*-alkanes in soils of the Dorokawa catchment. Hydrogen isotopic  
479 compositions of *n*-alkanes discriminate forest- and wetland soil-derived *n*-alkanes, which  
480 showed higher and lower values, respectively. A  $\delta^{13}C$  vs.  $\delta D$  diagram clearly indicates that  
481  $C_{25}$ - $C_{31}$  *n*-alkanes preserved in offshore sediments are largely derived from forest plants rather  
482 than wetland vegetation. This study demonstrates that the hydrogen isotopic composition of  
483 organic compounds provides a useful tool for inferring their source and delivery processes in  
484 a natural catchment system dominated by  $C_3$  plants.

485  
486  
487  
488  
489  
490  
491  
492  
493  
494  
495  
496  
497  
498  
499  
500  
501  
502  
503  
504  
505  
506  
507  
508  
509  
510  
511  
512  
513  
514  
515  
516  
517  
518  
519  
520  
521  
522  
523  
524  
525  
526  
527  
528  
529  
530  
531  
532  
533

## ACKNOWLEDGEMENT

This research is in part supported by the 21st-Century Center of Excellence Program funded by Ministry of Education Culture, Sports, Science and Technology. We thank James Bendle and Jeff Seewald for critical comments and corrections on previous versions of this manuscript. We also acknowledge the reviewers for critical comments on previous versions of this manuscript.

## REFERENCES

- Baas, M., Pancost, R., van Geel, B. and Sinninghe Damsté, J. S. (2000) A comparative study of lipids in *Sphagnum* species. *Org. Geochem.* **31**, 535–541.
- Bendle, J., Kawamura, K. and Yamazaki, K. (2006) Seasonal changes in stable carbon isotopic composition of *n*-alkanes in the marine aerosols from the western North Pacific: Implications for the source and atmospheric transport *Geochem. Cosmochim. Acta* **70**, 13-26.
- Bendle, J., Kawamura, K., Yamazaki, K., and Niwai, T. (2007) Latitudinal distribution of terrestrial lipid biomarkers and *n*-alkane compound specific stable carbon isotope ratios in the atmosphere over the western Pacific and Southern Ocean. *Geochim. Cosmochim. Acta* **71**, 5934-5955.
- Bi, X., Sheng, G., Liu, X., Li, C. and Fu, J. (2005) Molecular and carbon and hydrogen isotopic composition of *n*-alkanes in plant leaf waxes. *Org. Geochem.* **36**, 1405–1417.
- Bird, M.I., Summons, R.E., Gagan, M.K., Roksandic, Z., Dowling, L., Head, J., Fifield, L.K., Cresswell, R.G. and Johnson, D.P. (1995) Terrestrial vegetation change inferred from *n*-alkane  $\delta^{13}\text{C}$  analysis in the marine-environment. *Geochim. Cosmochim. Acta* **59**, 2853–2857.
- Bray E. E. and Evans E. D. (1961) Distribution of *n*-paraffins as a clue to recognition of source beds. *Geochim. Cosmochim. Acta* **36**, 1185-1203.
- Chikaraishi Y. and Naraoka, H. (2003) Compound-Specific  $\delta\text{D}$ - $\delta^{13}\text{C}$  analyses of *n*-alkanes extracted from terrestrial and aquatic plants. *Phytochem.* **63**, 361-371, 2004.
- Chikaraishi, Y. and Naraoka, H. (2005)  $\delta^{13}\text{C}$  and  $\delta\text{D}$  identification of sources of lipid biomarkers in sediments of Lake Haruna (Japan). *Geochim. Cosmochim. Acta* **69**, 3285–3297.
- Chikaraishi, Y., Yamada, Y. and Naraoka, H. (2005) Carbon and hydrogen isotope compositions of sterols from riverine and marine sediments. *Limnol. Oceanogr.* **50**, 1763-1770.
- Chikarasishi, Y. and Naraoka, H. (2006) Carbon and hydrogen isotope variation of plant biomarkers in a plant–soil system. *Chem. Geol.* **231**, 190-202.
- Collister, J.W., Rieley, G., Stern, B., Eglinton, G. and Fry, B. (1994) Compound-specific  $\delta^{13}\text{C}$  analyses of leaf lipids from plants with differing carbon dioxide metabolisms. *Org. Geochem.* **21**, 619–627.
- Dansgaard, W. (1964) Stable isotopes in precipitation. *Tellus* **16**, 436-468.
- Cranwell, P.A. (1973) Chain-length distribution of *n*-alkanes from lake sediments in relation to post-glacial environmental change. *Freshwater Biology* **3**, 259-265.
- Dawson, D., Crice, K. and Alexander, R. (2005) Effect of maturation on the indigenous  $\delta\text{D}$  signatures of individual hydrocarbons in sediments and crude oils from the Perth Basin (western Austria). *Org. Geochem.* **36**, 95-104.
- Eglinton, G. and Halimton, R.J. (1967) Leaf epicuticular waxes. *Science* **156**, 1322-1334.
- Ehleringer, J.P. and Rundel P.W. (1989) Stable Isotopes in Ecological Research. edited by P. W. Rundel, et a., 120 pp., Springer-Verlag.

- 534 Fernandes, M.A. and Sicre, M.-A. (2000) The importance of terrestrial organic carbon inputs  
535 on Kara Sea shelves as revealed by *n*-alkanes, OC and  $\delta^{13}\text{C}$  values. *Org. Geochem.* **31**,  
536 363–374.
- 537 Ficken, K.J., Barber, K.E. and Eglinton, G. (1998) Lipid biomarker and plant macrofossil  
538 stratigraphy of a Scottish montane peat bog over the last two millennia. *Org. Geochem.* **28**,  
539 217-237.
- 540 Ficken, K.J., Li, B., Swain, D.L. and Eglinton, G. (2000) An *n*-alkane proxy for the  
541 sedimentary inputs of submerged/floating freshwater aquatic macrophytes. *Org. Geochem.*  
542 **31**, 745-749.
- 543 Gagosian, R.B. and Peltzer, E.T. (1986) The importance of atmospheric input of terrestrial  
544 organic material to deep sea sediments. *Org. Geochem.* **10**, 661–669.
- 545 Goñi, M.A., (1997) Record of terrestrial organic matter composition in Amazon Fan  
546 sediments. *Proc. ODP Sci. Res.* **155**, 519– 530.
- 547 Goñi, M.A. Ruttenger, K.C. and Eglinton, T.I. (1997) Source and contribution of terrigenous  
548 organic carbon to surface sediments in the Gulf of Mexico. *Nature* **389**, 275-278.
- 549 Goñi, M.A. Ruttenger, K.C. and Eglinton, T.I. (1998) A reassessment of the sources and  
550 importance of land-derived organic matter in surface sediments from the Gulf of Mexico.  
551 *Geochim. Cosmochim. Acta* **62**, 3055-3075.
- 552 Hinrichs, K.-U., Rinna, J. and Rullkötter, J. (1998) Late Quaternary paleoenvironmental  
553 conditions indicated by marine and terrestrial molecular biomarkers in sediments from the  
554 Santa Barbara basin. In: Wilson, R.C., Tharp, V.L. (Eds.), Proceedings of the Fourteenth  
555 Annual Pacific Climate (PACLIM) Workshop, pp. 125-133.
- 556 Hou, J., Huang, Y., Wang, Y., Shuman, B., Oswald, W.W., Faison, E. and Foster, D.R. (2006)  
557 Post glacial climate reconstruction based on compound-specific D/H ratios of fatty acids  
558 from Blood Pond, New England. *Geochem. Geophys. Geosys.* **7**, 2005GC001076.
- 559 Hou, J., D'Andrea, W.J., MacDonald, D. and Huang, Y. (2007) Hydrogen isotopic variability  
560 in leaf waxes among terrestrial and aquatic plants around Blood Pond, Massachusetts  
561 (USA). *Org. Geochem.* **38**, 977–984.
- 562 Huang, Y.S., Bol, R., Harknes, D.D., Ineson, P. and Eglinton, G. (1996) Post-glacial variations  
563 in distributions,  $^{13}\text{C}$  and  $^{14}\text{C}$  contents of aliphatic hydrocarbons and bulk organic matter in  
564 three types of British upland soils. *Org. Geochem.* **24**, 273-287.
- 565 Huang, Y.S., Dupont, L., Sarnthein, M., Hayes, J.M. and Eglinton, G. (2000) Mapping of C4  
566 plant input from North West Africa into North East Atlantic sediments. *Geochim.*  
567 *Cosmochim. Acta* **64**, 3505– 3513.
- 568 Huang, Y.S., Freeman, K.H., Eglinton, T.I. and Street-Perrott, F.A. (2001) Climate change as  
569 the dominant control on glacial–interglacial variations in C3 and C4 plant abundance.  
570 *Science* **293**, 1647–1651.
- 571 Huang, Y., Shuman, B., Wang Y. and Webb, T. (2004) Hydrogen isotope ratios of individual  
572 lipids in lake sediments as novel tracers of climatic and environmental change: a surface  
573 sediment test. *J. Paleolimnol.* **31**, 363–375.
- 574 Huang, Y., Shuman, B., Wang, Y., Webb III, T., Grimm, E.C. and Jacobson Jr. G.L. (2006)  
575 Climatic and environmental controls on the variation of C3 and C4 plant abundances in  
576 central Florida for the past 62,000 years. *Palaeogeogr. Palaeoclimatol. Palaeoecol.* **237**,  
577 428-435.
- 578 Jacob, J., Huang, Y., Disnar, J.-R., Sifeddine, A., Boussafir, M., Albuquerque A.L.S. and  
579 Turcq, B. (2007) Paleohydrological changes during the last deglaciation in Northern Brazil.  
580 *Quat. Sci. Rev.* **26**, 1004-1015.
- 581 Jaffé, R., Wolf, G.A., Cabrera, A.C. and Chitty, H.C. (1995) The biogeochemistry of lipids in  
582 rivers of the Orinoco Basin. *Geochim. Cosmochim. Acta* **59**, 4507-4522.
- 583 Kawamura, K., Ishimura, Y. and Yamazaki, K. (2003) Four year observations of terrestrial

- 584 lipid class compounds in marine aerosols from the western North Pacific. *Global*  
585 *Biogeochem. Cycles* **17**, doi:10.1029/2001GB001810.
- 586 Keeling C.D., Carter A.F. and Mook W. G. (1984) Seasonal, latitudinal, and secular  
587 variations in the abundance and isotopic ratios of atmospheric CO<sub>2</sub>. 2. Results from  
588 oceanographic cruises in the tropical Pacific Ocean. *J. Geophys. Res.* **89**, 4615-4628.
- 589 Keil, R.G., Tsamakis, E., Bor Fuh, C., Giddings, J.C. and Hedges, J.I. (1994) Mineralogical  
590 and textural controls on the organic composition of coastal marine sediments:  
591 hydrodynamic separation using SPLITT-fractionation. *Geochim. Cosmochim. Acta* **58**,  
592 879-893.
- 593 Kurill, E., Sachse, D., Mügler, I., Thiele, A. and Gleixner, G. (2006) Compound-specific  $\delta^{13}\text{C}$   
594 and  $\delta^2\text{H}$  analyses of plant and soil organic matter: A preliminary assessment of the effects  
595 of vegetation change on ecosystem hydrology. *Soil Biol. Biochem.* **38**, 3211-3221.
- 596 Lehtonen, K. and Ketola, M. (1993) Solvent-extractable lipids of *Shagnum*, *Carex*, *Bryales*  
597 and *Carex-Bryales* peats: content and compositional features vs. peat humification. *Org.*  
598 *Geochem.* **20**, 363-380.
- 599 Liu, W. and Huang, Y. (2005) Compound specific D/H ratios and molecular distributions of  
600 higher plant leaf waxes as novel paleoenvironmental indicators in the Chinese Loess  
601 Plateau. *Org. Geochem.* **36**, 851-860.
- 602 Liu, W., Yang, H. and Li, L. (2006) Hydrogen isotopic compositions of *n*-alkanes from  
603 terrestrial plants correlate with their ecological life forms. *Oecologia* **150**, 330-338.
- 604 Mead, R., Xu, Y., Chong, J. and Jaffé, R. (2005) Sedimentary and soil organic matter source  
605 assessment as revealed by the molecular distribution and carbon isotopic composition of  
606 *n*-alkanes. *Org. Geochem.* **36**, 363-370.
- 607 Nichols, J.E., Booth, R.K. and Jackson, S.T. (2006) Paleohydrologic reconstruction based on  
608 *n*-alkane distributions in ombrotrophic peat. *Org. Geochem.* **37**, 1505-1513.
- 609 Nott, C.J., Xie, S., Avsejs, L.A., Maddy, D., Chambers, F.M. and Evershed, R.P. (2000)  
610 *n*-Alkane distributions in ombrotrophic mires as indicators of vegetation change related to  
611 climatic variations. *Org. Geochem.* **31**, 231-235.
- 612 Ogawa, A., Shibata, H., Suzuki, K., Mitchell, M.J. and Ikegami, Y. (2006) Relationship of  
613 topography to surface water chemistry with particular focus on nitrogen and organic  
614 carbon solutes within a forested watershed in Hokkaido, Japan. *Hydrolog. Proces.* **20**,  
615 251-265.
- 616 Pancost, R.D. and Boot, C.S. (2004) The palaeoclimatic utility of terrestrial biomarkers in  
617 marine sediments. *Mar. Chem.* **92**, 239-261.
- 618 Prahl, F.G., Ertel, J.R., Goni, M.A., Sparrow, M.A. and Eversmeyer, B. (1994) Terrestrial  
619 organic carbon contribution to sediments on the Washington margin. *Geochim.*  
620 *Cosmochim. Acta* **58**, 3035-3048.
- 621 Pedentchouk, N., Sumner, W., Tipple, B. and Pagani, M. (2008)  $\delta^{13}\text{C}$  and  $\delta\text{D}$  compositions of  
622 *n*-alkanes from modern angiosperms and conifers: An experimental set up in central  
623 Washington State, USA. *Org. Geochem.* **39**, 1066-1071.
- 624 Rieley, G., Collier, R.J., Jones, D.M., Eglinton, G., Eakin, P.A. and Fallick, A.E. (1991)  
625 Sources of sedimentary lipids deduced from stable carbon-isotope analyses of individual  
626 compounds. *Nature* **352**, 425-427.
- 627 Rommerskirchen, F., Plader, A., Eglinton, G., Chikaraishi, Y. and Rullkötter, J. (2006)  
628 Chemotaxonomic significance of distribution and stable isotopic composition of  
629 long-chain alkanes and alkan-1-ols in C<sub>4</sub> grass waxes. *Org. Geochem.* **37**, 1303-1332.
- 630 Sachse, D., Radke, J. and Gleixner, G. (2004) Hydrogen isotope ratios of recent lacustrine  
631 sedimentary *n*-alkanes record modern climate variability. *Geochim. Cosmochim. Acta* **68**,  
632 4877-4889.
- 633 Sachse, D., Radke, J. and Gleixner, G. (2006)  $\text{dD}$  values of individual *n*-alkanes from

- 634 terrestrial plants along a climatic gradient – Implications for the sedimentary biomarker  
635 record. *Org. Geochem.* **37**, 469-483.
- 636 Schefub, E., Schouten, S. and Schneider, R.R. (2005) Climatic controls on central African  
637 hydrology during the past 20,000 years. *Nature* **437**, 1003-1006.
- 638 Seki, O., Kawamura, K., Nakatsuka, T., Ohnishi, K., Ikehara, M. and Wakatsuchi, M. (2003)  
639 Sediment core profiles of long-chain *n*-alkanes in the Sea of Okhotsk: Enhanced transport  
640 of terrestrial organic matter from the last deglaciation to the early Holocene. *Geophys. Res.*  
641 *Lett.* **30**, 2001GL014464.
- 642 Seki, O., Yoshikawa, C., Nakatsuka, T., Kawamura, K. and Wakatsuchi, M. (2006) Fluxes,  
643 source and transport of organic matter in the western Sea of Okhotsk: Stable carbon  
644 isotopic ratios of *n*-alkanes and total organic carbon. *Deep-Sea Res. I* **53**, 253–270.
- 645 Seki, O., Meyers, P.A., Kawamura, K., Zheng, Y. and Zhou, W. (2009) Hydrogen isotopic  
646 ratios of plant-wax *n*-alkanes in a peat bog deposited in northeast China during the last 16  
647 kyr. *Org. Geochem.* **40**, 671-677.
- 648 Sessions, A. L., Burgoyne, T. W., Schimmelmann, A. and Hayes, J.M. (1999) Fractionation of  
649 hydrogen isotope in lipid biosynthesis. *Org. Geochem.* **30**, 1193-1200.
- 650 Sessions, A.L. Burgoyne, T.W., Schimmelmann, A. and Hayes, J.M. (2001) Corrections of H<sub>3</sub><sup>+</sup>  
651 contributions in hydrogen isotope ratio monitoring mass spectrometry. *Anal. Chem.* **73**,  
652 192-199.
- 653 Shuman, B., Huang, Y. and Newby, P. (2006) Compound-specific isotopic analyses track  
654 changes in seasonal precipitation regimes in the Northeastern United States. *Quat. Sci. Rev.*  
655 **25**, 2992-3002.
- 656 Smith, B.N. and Epstein S. (1971) Two categories of <sup>13</sup>C/<sup>12</sup>C ratios for higher plants. *Plant*  
657 *Physiol.* **47**, 380-384.
- 658 Sternberg, L., Deniro, M.J. and Ajie H. (1984) Hydrogen isotope ratios of saponifiable lipids  
659 and cellulose nitrate from CAM, C3 and C4 plants. *Phytochem.* **23**, 2475-2477.
- 660 Xie, S., Nott, C. J., Avsejs, L. A., Volders, F., Maddy, D., Chambers, F. M., Gledhill, A., Carter,  
661 J. F. and Evershed, R. P. (2000) Paleoclimate records in compound-specific δD values of  
662 a lipid biomarker in ombrotrophic peat. *Org. Geochem.* **31**, 1053-1057.
- 663 Xie, S., Nott, C. J., Avsejs, L. A., Maddy, D., Chambers, F. M. and Evershed, R.P. (2004)  
664 Molecular and isotopic stratigraphy in an ombrotrophic mire of paleoclimate  
665 reconstruction. *Geochem. Cosmochim. Acta* **68**, 2849-2862.
- 666 Xiao-niu, Z. and Shibata, H. (2007) Landscape patterns of overstory litterfall and related  
667 nutrient fluxes in a cool-temperate forest watershed in northern Hokkaido, Japan. *J. Forest.*  
668 *Res.* **18**, 249-254.
- 669 Yamada, K. and Ishiwatari, R. (1999) Carbon isotopic compositions of long-chain *n*-alkanes  
670 in the Japan Sea sediments: implications for paleoenvironmental changes over the past 85  
671 kyr. *Org. Geochem.* **30**, 367-377.
- 672 Yang, H. and Huang, Y. (2003) Preservation of lipid hydrogen isotope ratios in Miocene  
673 lacustrine sediments and plant fossils at Clarkia, northern Idaho, USA. *Org. Geochem.* **34**,  
674 413-423.
- 675 Zheng, Y., Zhou, W., Meyers, P.A. and Xie, S. (2007) Lipid biomarkers in the  
676 Zoige-Hongyuan peat deposit: Indicators of Holocene climate changes in West China. *Org.*  
677 *Geochem.* **38**, 1927-1940.
- 678

Table 1 Concentration and molecular distribution of *n*-alkanes in Dorokawa catchment

Site	Depth (cm)	Molecular distribution				
		Conc. ( $\mu\text{g/g}$ )	CPI <sup>a</sup>	ACL <sup>b</sup>	$C_{27}/C_{31}$ <sup>c</sup>	$P_{aq}$ <sup>d</sup>
Site A-1 (forest)	0-5 cm	28.8	6.2	29.1	0.68	0.22
Site A-2 (forest)	0-5 cm	50.7	8.5	29.9	0.53	0.14
Site A-3 (forest)	0-10 cm	173.5	9.8	29.7	0.55	0.14
Site A-3 (forest)	10-20 cm	24.1	5.9	30.3	0.62	0.21
Site A-3 (forest)	20-30 cm	7.0	5.5	29.2	0.70	0.23
Site A-3 (forest)	50-60 cm	7.5	5.0	28.8	0.35	0.24
Site A-3 (forest)	80-90 cm	0.5	7.0	29.5	0.40	0.19
Site B-1 (forest)	0-5 cm	23.7	6.1	28.7	0.96	0.19
Site B-2 (forest)	0-5 cm	28.4	5.7	30.8	0.20	0.13
Site B-3 (forest)	0-10 cm	20.1	5.7	28.8	0.96	0.24
Site B-3 (forest)	40-50 cm	5.4	6.2	28.9	0.62	0.20
Site B-3 (forest)	80-90 cm	8.4	8.4	28.9	0.59	0.22
Site C-1 (forest)	0-5 cm	21.5	4.4	28.3	1.25	0.35
Site C-2 (forest)	0-5 cm	30.4	6.5	28.4	0.90	0.23
Site C-3 (forest)	0-10 cm	25.1	5.1	27.7	1.18	0.40
Site C-3 (forest)	10-20 cm	22.9	4.7	28.7	0.96	0.22
Site C-3 (forest)	20-30 cm	12.7	4.8	28.6	0.91	0.22
Site C-3 (forest)	30-40 cm	4.1	5.0	28.4	0.91	0.27
Site C-3 (forest)	40-50 cm	7.0	6.7	28.6	0.60	0.27
Site C-3 (forest)	50-60 cm	7.3	7.0	29.1	0.53	0.18
Site C-3 (forest)	60-70 cm	6.5	7.6	29.2	0.48	0.18
Site C-3 (forest)	70-80 cm	4.6	7.7	29.1	0.50	0.19
Site C-3 (forest)	80-90 cm	4.8	8.7	29.3	0.34	0.16
Site D (wetland)	0-30 cm	57.4	6.9	29.9	0.28	0.12
Site D (wetland)	30-60 cm	204.2	8.9	30.5	0.10	0.28
Site D (wetland)	60-90 cm	90.7	8.4	30.3	0.09	0.17
Site D (wetland)	90-120 cm	428.9	7.1	30.1	0.16	0.14
Site D (wetland)	120-150 cm	215.5	5.1	29.8	0.22	0.15
Site E-1 (wetland)	0-10 cm	142.1	6.6	28.1	0.78	0.44
Site E-1 (wetland)	10-20 cm	51.6	6.0	28.4	0.67	0.39
Site E-1 (wetland)	20-30 cm	224.4	6.3	28.5	0.64	0.42
Site E-1 (wetland)	30-40 cm	138.8	5.4	28.1	0.88	0.38
Site E-1 (wetland)	60-70 cm	12.1	4.6	28.4	0.34	0.29
Site E-2 (wetland)	0-10 cm	276.5	7.7	29.7	0.29	0.22
Site E-2 (wetland)	40-50 cm	237.7	6.2	28.6	0.43	0.34
Site F-1 (wetland)	0-10 cm	123.2	7.5	30.0	0.25	0.14
Site F-1 (wetland)	10-20 cm	435.0	8.0	30.9	0.07	0.07
Site F-1 (wetland)	20-30 cm	103.2	7.8	30.2	0.11	0.17
Site F-1 (wetland)	70-80 cm	24.3	6.1	31.7	0.25	0.20
Site F-1 (wetland)	110-120 cm	71.7	7.7	30.8	0.31	0.11
Site F-2 (wetland)	0-10 cm	67.7	8.3	30.6	0.13	0.09
Site G (estuary)	0-5 cm	30.4	7.9	28.8	0.87	0.23
Site H (lake)	0-5 cm	35.8	7.3	28.3	1.34	0.27
Site I (lake)	0-5 cm	10.4	7.4	27.9	1.62	0.31

(a) CPI, carbon preference index, =  $2\sum_{\text{odd}} C_{23}-C_{33}/(\sum_{\text{even}} C_{22}-C_{34}+\sum_{\text{even}} C_{24}-C_{36})$ .(b) ACL, average chain length, =  $(23*C_{23}+25*C_{25}+27*C_{27}+29*C_{29}+31*C_{31}+33*C_{33}+35*C_{35})/\sum_{\text{odd}} C_{23}-C_{35}$ .(c)  $C_{27}/C_{31}$ , proportion of  $C_{27}$  to  $C_{31}$ .(d)  $P_{aq}$ , proportion of aquatic plant *n*-alkane, =  $(C_{23}+C_{25})/(C_{23}+C_{25}+C_{29}+C_{31})$ .

Table 2 Stable carbon isotopic compositions ( $\delta^{13}\text{C}$ ) of *n*-alkanes in Dorokawa catchment

Site	Depth (cm)	$\delta^{13}\text{C}$ (‰)											
		C <sub>23</sub>	S.D. <sup>a</sup>	C <sub>25</sub>	S.D. <sup>a</sup>	C <sub>27</sub>	S.D. <sup>a</sup>	C <sub>29</sub>	S.D. <sup>a</sup>	C <sub>31</sub>	S.D. <sup>a</sup>	C <sub>33</sub>	S.D. <sup>a</sup>
Site A-1 (forest)	0-5 cm			-33.0	0.5	-32.9	0.2	-34.2	0.3	-33.5	0.1	-35.1	0.2
Site A-2 (forest)	0-5 cm			-33.7	0.3	-33.3	0.1	-34.8	0.3	-34.4	0.0	-37.0	0.2
Site A-3 (forest)	0-5 cm			-32.9		-32.5		-34.0		-34.0		-36.0	
Site B-1 (forest)	0-5 cm			-33.4		-32.0		-33.5		-34.0		-34.5	
Site B-2 (forest)	0-5 cm			-34.9	0.3	-33.5	0.2	-34.6	0.1	-34.4	0.3	-33.5	0.1
Site B-3 (forest)	40-50 cm			-32.1		-32.9		-33.6		-33.1		-33.4	
Site B-3 (forest)	80-90 cm			-32.6		-32.5		-33.1		-33.2		-32.7	
Site C-2 (forest)	0-5 cm			-33.4	0.2	-33.1	0.2	-34.8	0.3	-35.6	0.2	-35.8	0.1
Site C-3 (forest)	10-20 cm			-32.8		-32.8		-35.3		-34.4		-35.6	
Site C-3 (forest)	20-30 cm			-32.6		-32.8		-34.9		-34.4		-35.5	
Site C-3 (forest)	40-50 cm			-31.7	0.2	-32.2	0.3	-33.3	0.3	-33.2	0.1	-34.0	0.4
Site C-3 (forest)	50-60 cm			-31.7		-32.3		-33.5		-33.0		-33.4	
Site C-3 (forest)	70-80 cm			-32.4		-32.3		-32.9		-32.5		-32.8	
Site D (wetland)	0-30 cm	-32.1		-33.0		-34.1		-36.4		-34.5		-34.2	
Site D (wetland)	30-60 cm	-32.7	0.1	-34.8	0.2	-32.2	0.3	-31.3	0.2	-31.5	0.2	-32.1	
Site D (wetland)	60-90 cm	-31.2		-31.7		-32.2		-33.3		-33.2		-34.8	
Site D (wetland)	90-120 cm	-32.0		-32.2		-33.3		-34.7		-33.2		-33.5	
Site D (wetland)	120-150 cm	-32.5	0.1	-32.9	0.0	-37.2	0.5	-35.9	0.5	-34.6	0.1	-34.7	0.4
Site E-1 (wetland)	0-10 cm	-35.2		-34.1		-34.4		-34.2		-34.5		-35.1	
Site E-1 (wetland)	10-20 cm	-34.7		-33.2		-33.5		-33.6		-33.7		-34.6	
Site E-1 (wetland)	20-30 cm	-34.0		-32.8	0.3	-33.2	0.1	-33.5	0.1	-33.9	0.4	-35.1	0.3
Site E-2 (wetland)	0-10 cm	-34.6		-34.3		-34.5		-34.2		-34.4		-35.0	
Site F-1 (wetland)	0-10 cm			-33.3		-32.9		-32.3		-32.3		-32.1	
Site F-1 (wetland)	10-20 cm	-32.6	0.3	-33.6	0.0	-32.1	0.1	-32.4	0.4	-32.6	0.2	-32.6	0.2
Site F-1 (wetland)	20-30 cm			-32.1		-32.7		-32.1		-32.2		-32.1	
Site F-1 (wetland)	110-120 cm	-33.4		-33.6		-33.4		-33.6		-33.7		-35.1	
Site F-2 (wetland)	0-10 cm	-32.6		-33.1		-33.7		-33.8		-33.4		-34.0	
Site G (estuary)	0-5 cm			-32.7	0.1	-32.2	0.3	-32.4	0.2	-32.8	0.2	-32.4	0.1
Site H (lake)	0-5 cm			-32.8		-32.6		-33.1		-33.2		-34.8	
Site I (lake)	0-5 cm	-31.7		-32.7		-33.0		-33.5		-33.7		-34.3	

(a) S.D., standard deviation



Table 3 Stable hydrogen isotopic compositions ( $\delta D$ ) of *n*-alkanes in Dorokawa catchment

Site	Depth (cm)	$\delta D$ (‰)											
		C <sub>23</sub>	S.D. <sup>a</sup>	C <sub>25</sub>	S.D. <sup>a</sup>	C <sub>27</sub>	S.D. <sup>a</sup>	C <sub>29</sub>	S.D. <sup>a</sup>	C <sub>31</sub>	S.D. <sup>a</sup>	C <sub>33</sub>	S.D. <sup>a</sup>
Site A-1 (forest)	0-5 cm			-211	1	-205	0	-203	2	-195	2	-203	1
Site A-2 (forest)	0-5 cm			-211	2	-202	3	-198	5	-194	5	-192	5
Site A-3 (forest)	0-5 cm			-211	1	-201	1	-195	3	-190	1	-204	0
Site B-1 (forest)	0-5 cm			-207	7	-214	4	-211	1	-202	4	-200	6
Site B-2 (forest)	0-5 cm			-210	2	-211	5	-203	2	-199	3	-198	2
Site B-3 (forest)	0-10 cm					-205	4	-212	0	-202	6		
Site B-3 (forest)	40-50 cm			-187	4	-204	8	-208	4	-203	3	-188	2
Site B-3 (forest)	80-90 cm												
Site C-1 (forest)	0-5 cm			-206	2	-208	4	-210	1	-198	0	-187	6
Site C-2 (forest)	0-5 cm			-206	1	-199	3	-195	0	-191	3	-190	9
Site C-3 (forest)	0-10 cm					-192		-213		-190			
Site C-3 (forest)	10-20 cm			-211	4	-214	5	-213	6	-197	4	-191	7
Site C-3 (forest)	20-30 cm			-202	4	-212	0	-214	1	-205	0	-196	2
Site C-3 (forest)	30-40 cm			-199		-198		-203		-191		-193	
Site C-3 (forest)	40-50 cm			-200	9	-197	1	-205	6	-199	1	-188	6
Site C-3 (forest)	50-60 cm			-201		-203		-203		-189		-196	
Site C-3 (forest)	60-70 cm			-203		-203		-186		-180		-197	
Site C-3 (forest)	70-80 cm			-196	5	-200	5	-207	3	-206	0	-186	8
Site C-3 (forest)	80-90 cm			-195	4	-203	4	-199	1	-200	7	-190	13
Site D (wetland)	0-30 cm		5	-214	2	-221	3	-216	0	-229	2	-230	1
Site D (wetland)	30-60 cm		2	-217	5		6	-224	1	-241	2	-232	2
Site D (wetland)	60-90 cm	-228		-221		-223		-208		-202			
Site D (wetland)	90-120 cm			-216	6	-216	1	-218	0	-242	1	-239	2
Site D (wetland)	120-150 cm			-216	5	-227	2	-222	2	-237	2	-236	2
Site E-1 (wetland)	0-10 cm	-227	4	-228	1	-222	1	-217	2	-219	7	-208	5
Site E-1 (wetland)	10-20 cm	-227	0	-233	4	-225	3	-225	7	-220	6	-217	5
Site E-1 (wetland)	20-30 cm	-239	1	-229	1	-220	3	-220	0	-212	1	-211	1
Site E-2 (wetland)	0-10 cm 2	-234	0	-237	4	-223	3	-221	3	-220	3	-222	3
Site E-2 (wetland)	40-50 cm 2	-239	4	-237	5	-221	3	-222	5	-219	3	-224	3
Site F-1 (wetland)	0-10 cm			-212		-210		-227		-240		-230	
Site F-1 (wetland)	10-20 cm					-231	2	-244	0	-240	0	-222	0
Site F-1 (wetland)	20-30 cm					-217	4	-240	1	-243	1		
Site F-1 (wetland)	110-120 cm			-223	2	-211	1	-219	1	-231	3	-219	1
Site F-2 (wetland)	0-10 cm			-231	0	-231	4	-229	1	-241	1	-235	2
Site G (estuary)	0-5 cm	-217	3	-219	1	-217	1	-216	2	-214	2	-213	1
Site H (lake)	0-5 cm			-203	1	-201	6	-202	6	-196	4		5
Site I (lake)	0-5 cm	-207	2	-202	1	-203	1	-204	0	-196	0		

(a) S.D., standard deviation

**FIGURE CAPTIONS**

682

683

684 Figure 1. Sampling locations in the Dorokawa River watershed and northern part of Lake  
685 Shumarinai. Solid circles and triangles represent forest sampling sites (Sites A, B and C) and  
686 wetland (Sites D, E and F) soils, respectively. Solid squares represent surface sediment  
687 sampling sites in the river and lake (Sites G, H and I). Open circles show river water sampling  
688 sites (Sites 1, 4, 6, 10, 13, 16 and 20). Parenthetical numeric numbers indicate the altitude of  
689 soil sampling points. The shaded area in the watershed is the wetland area.

690

691 Figure 2. Seasonal changes in hydrogen isotopic compositions of river water ( $\delta D_{RW}$ ) in the  
692 Dorokawa watershed during the period from July 2003 to October 2004. River water  
693 sampling sites are shown in Figure 1.

694

695 Figure 3. Typical molecular distributions of *n*-alkanes in the forest (Sites A-C), wetland (Sites  
696 D-F) and lake (Sites G-I) samples in the Dorokawa catchment system and Lake Shumarinai.

697

698 Figure 4. Depth profiles of concentration, carbon preference index (CPI), average chain  
699 length (ACL),  $C_{27}/C_{31}$  and  $P_{aq}$  of *n*-alkanes in forest soils (Sites A-C) and wetland peat (Sites  
700 D-F) and lake sediments (Sites G-I). Data for lake surface sediments are represented by  
701 shaded vertical bands in the figures.

702

703 Figure 5. Depth profiles of stable carbon isotopic compositions ( $\delta^{13}C$ ) of  $C_{25}$ - $C_{33}$  odd carbon  
704 number *n*-alkanes in forest (Sites A-C), wetland (Sites D-F) and lake (Sites G-I) samples in  
705 the Dorokawa catchment system and Lake Shumarinai. Data in lake surface sediments are  
706 represented by shaded vertical bands in the figures. Bars in the figures represent standard  
707 deviations.

708

709 Figure 6. Depth profiles of the hydrogen isotopic compositions ( $\delta D$ ) of  $C_{25}$ - $C_{33}$  odd carbon  
710 number *n*-alkanes in forest (Sites A-C), wetland (Sites D-F) and lake (Sites G-I) samples in

711 the Dorokawa catchment system and Lake Shumarinai. Data in lake surface sediments are  
712 represented by shaded vertical bands in the figures. Bars in the figures represent standard  
713 deviations.

714

715 Figure 7.  $C_{27}/C_{31}$  vs.  $P_{aq}$  diagrams of *n*-alkanes in the Dorokawa catchment system and Lake  
716 Shumarinai.

717

718 Figure 8.  $\delta^{13}C$  vs.  $\delta D$  diagrams for odd  $C_{25}$ - $C_{33}$  *n*-alkanes in the Dorokawa catchment system  
719 and Lake Shumarinai. Bars in the figures represent standard deviations.

Figure 1 (Seki et al.)

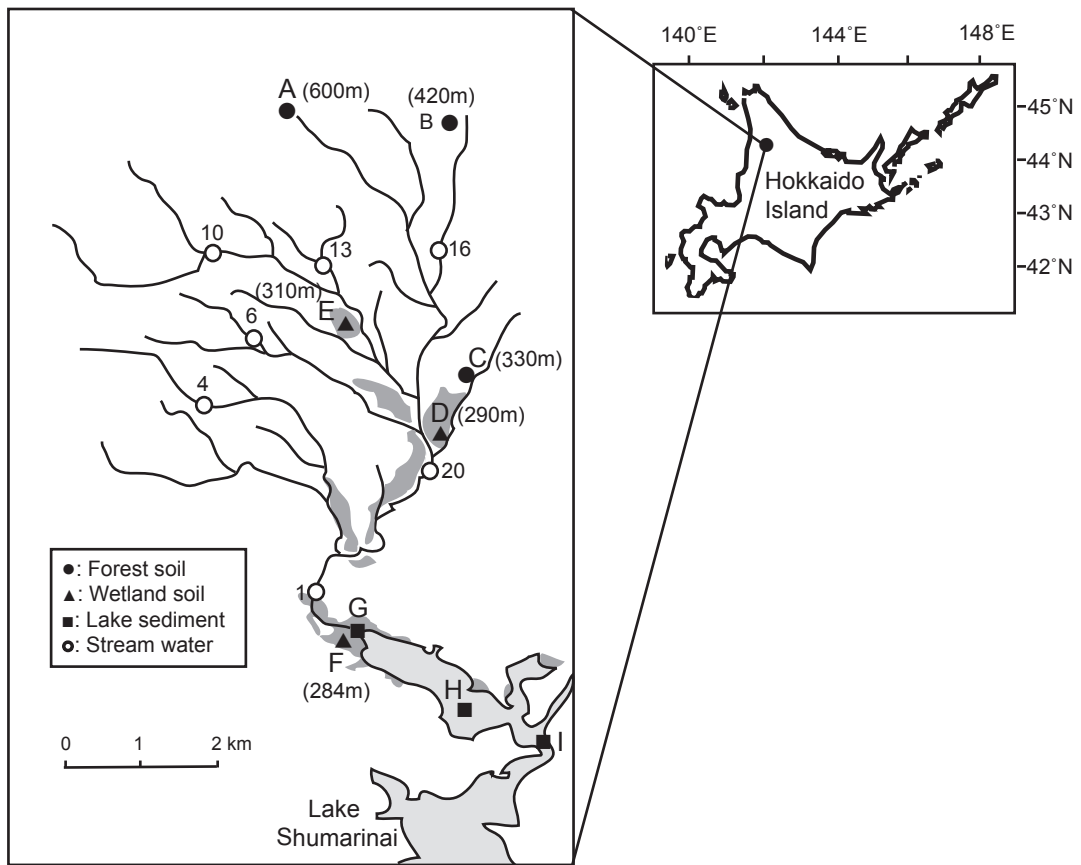


Figure 2 (Seki et al.)

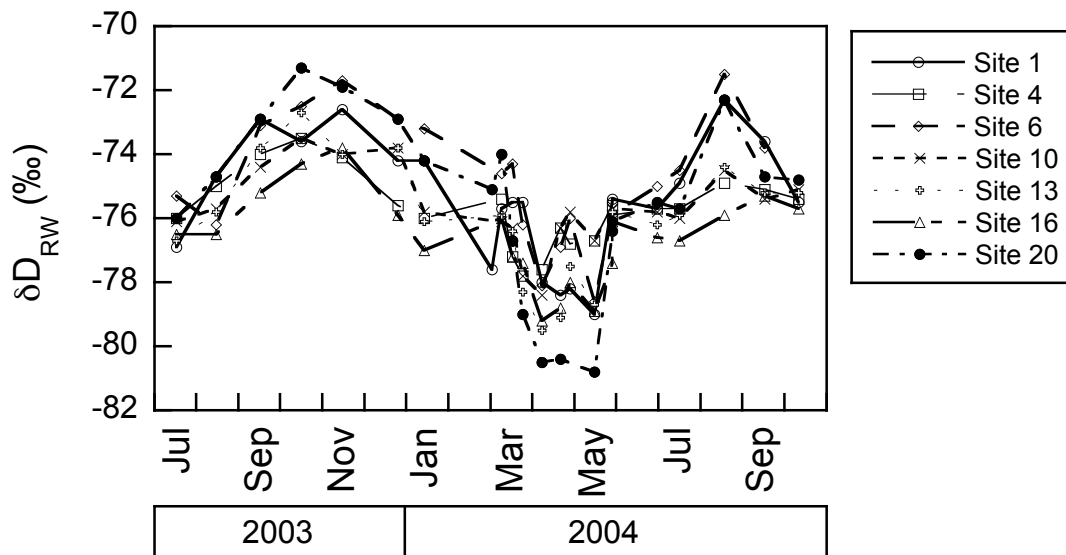


Figure 3 (Seki et al.)

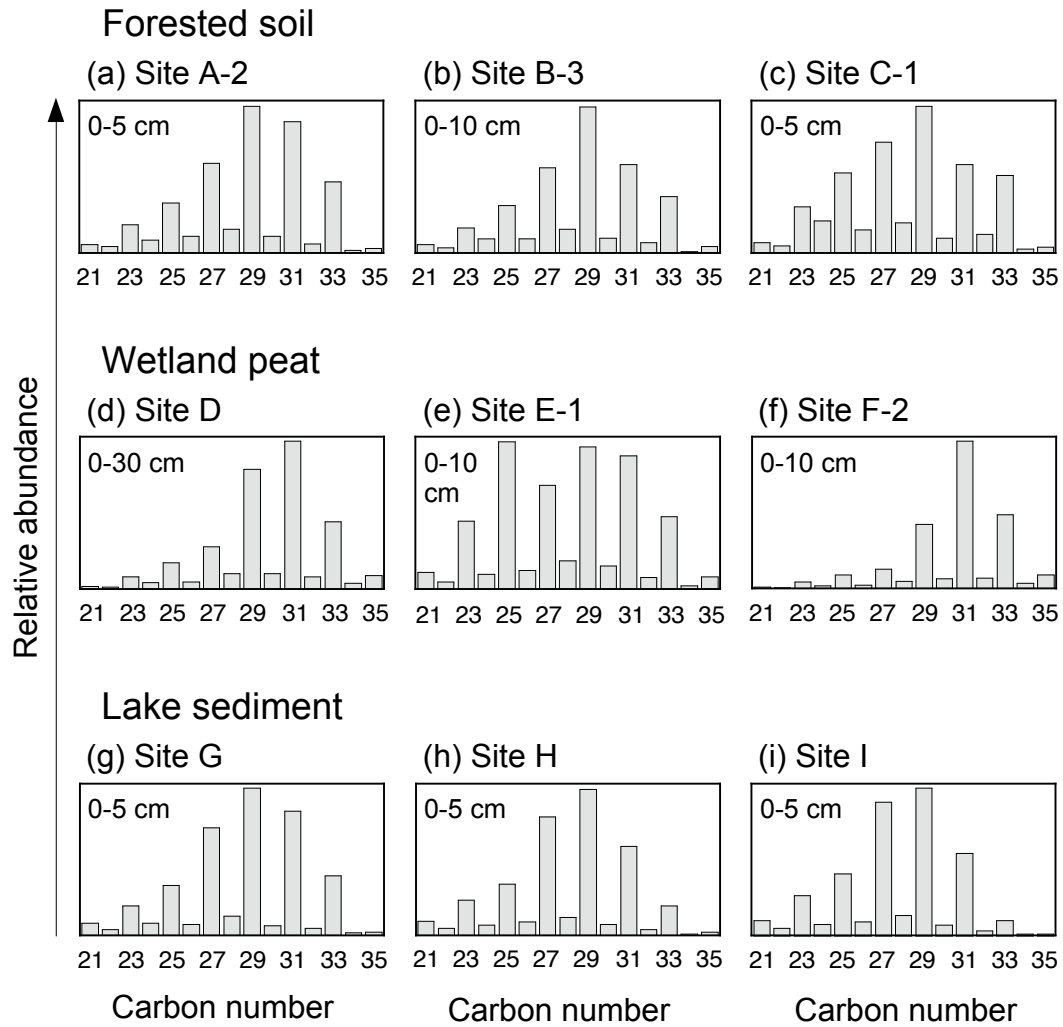


Figure 4 (Seki et al.)

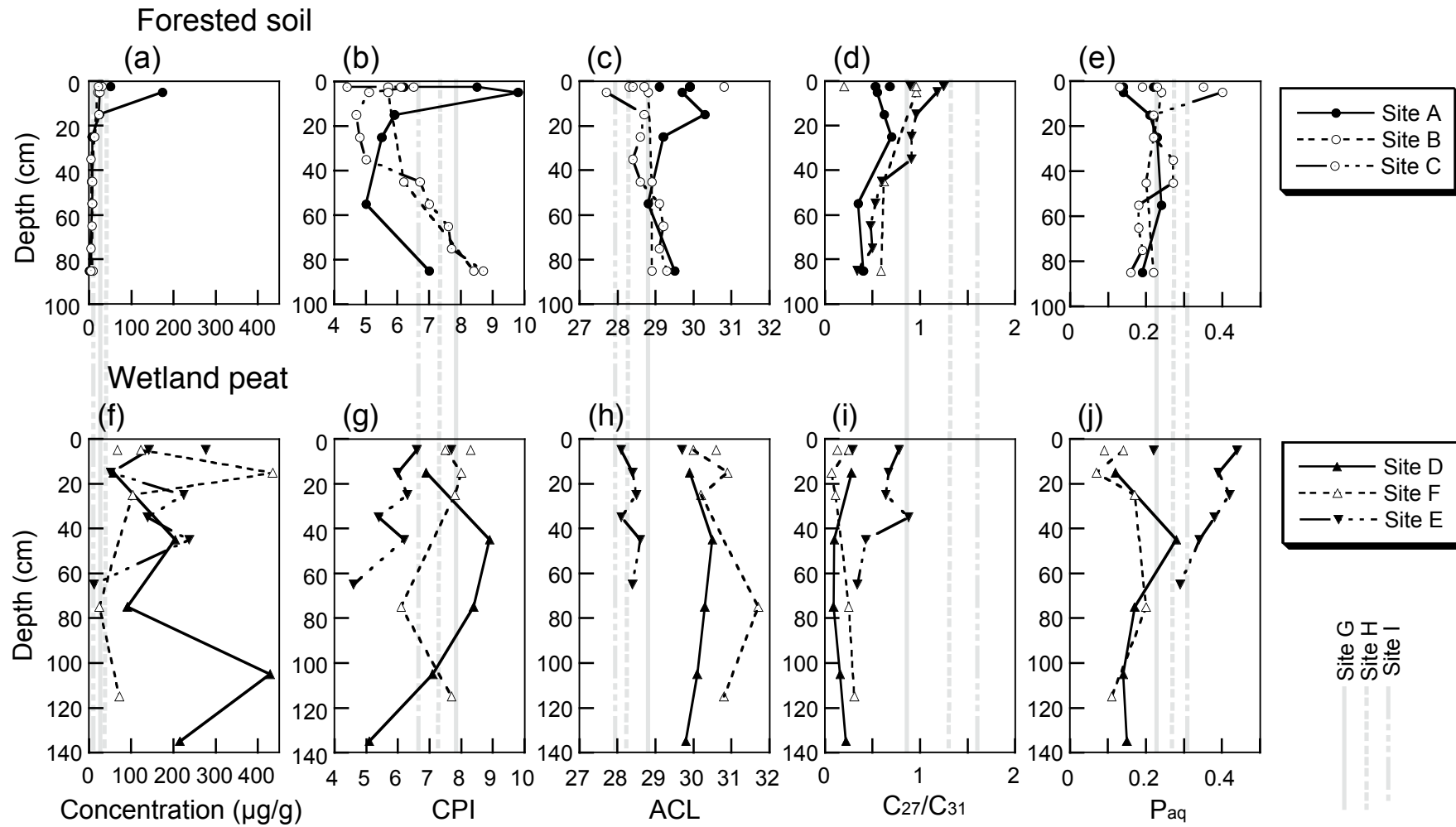
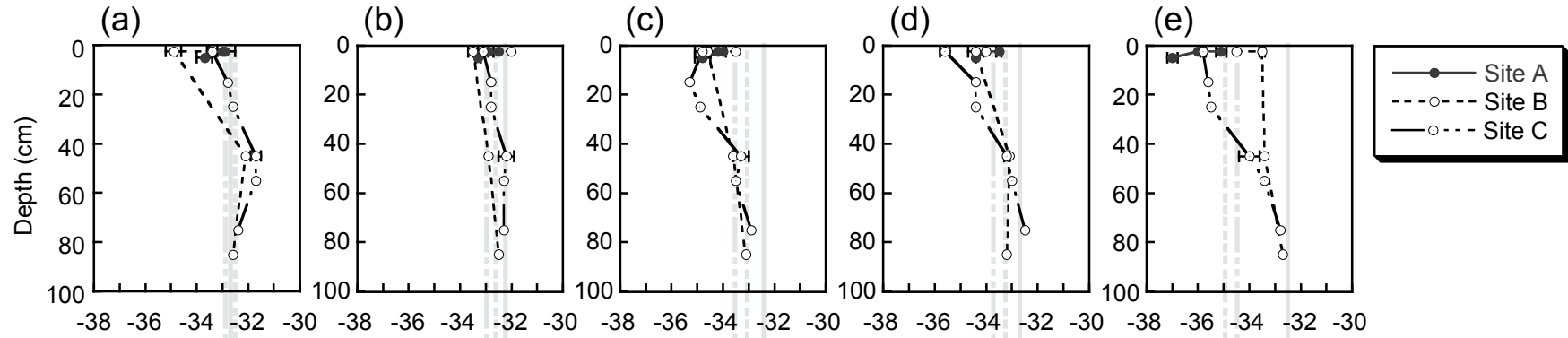


Figure 5 (Seki et al.)

Forested soil



Wetland peat

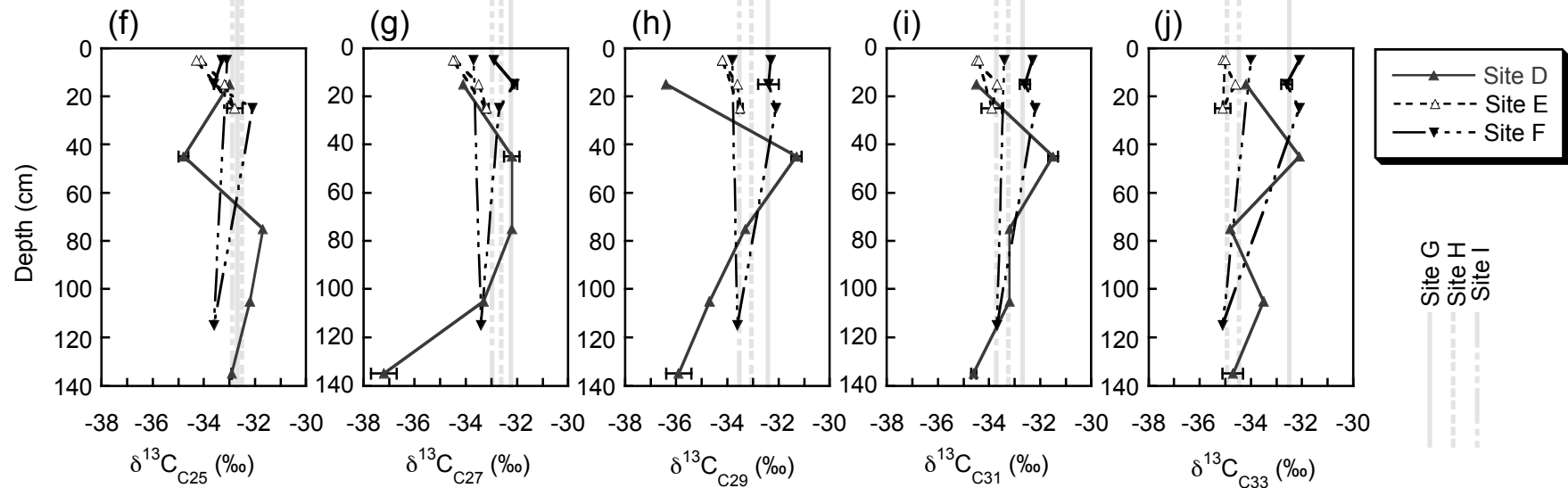
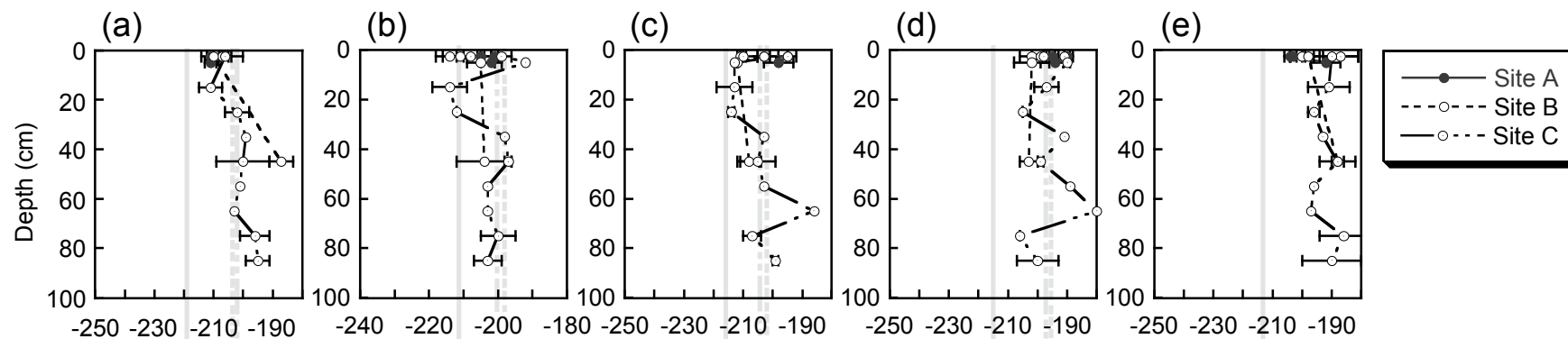




Figure 6 (Seki et al.)

Forested soil



Wetland peat

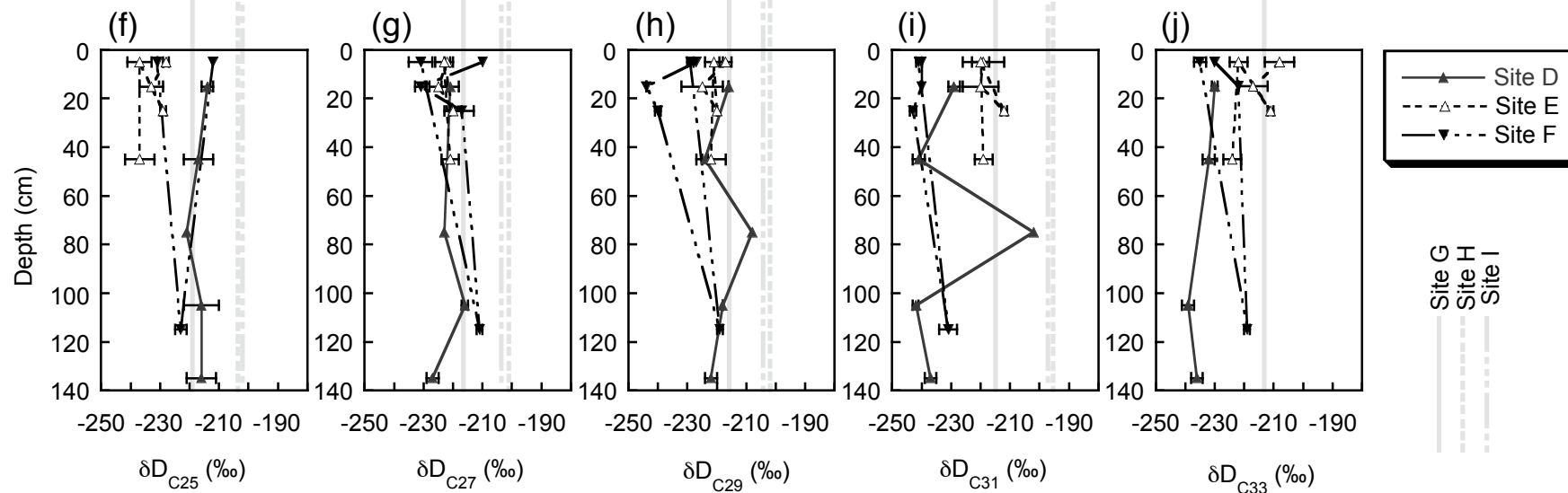


Figure 7 (Seki et al.)

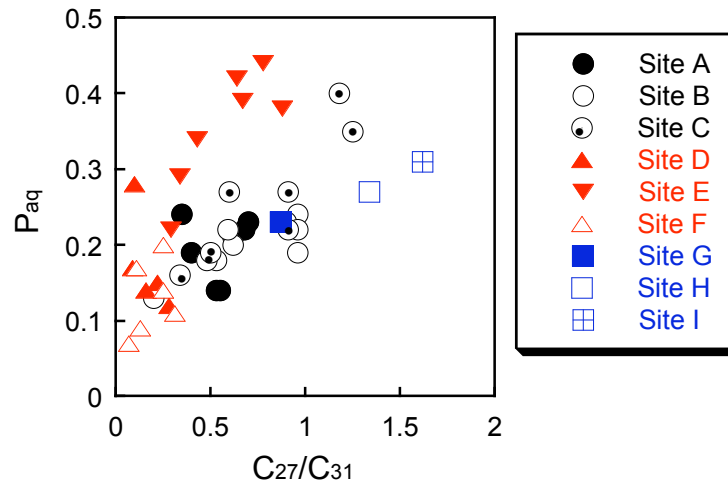


Figure 8 (Seki et al.)

